UNEC Journal of Engineering and Applied Sciences **SECTION:**
Vol. 6, No.1, 2026, pp. 5-11 **ENGINEERING**
DOI: https://doi.org/10.61640/ujeas.2026.0501 **SCIENCES**

The effect of disc material on the mechanical performance of brake pads during single-stop braking

M. Chaqouri[1*], M. Maniana[1], F. Erchiqui[2], A. Tajmouati[1]

[1]Hassan First University, Faculty of Sciences and Techniques, Settat 26000, Morocco*
[2]UQAT, University of Quebec in Abitibi Timiskaming, 445 boulevard de l'Universite Rouyn-Noranda, Canada
email: *m.chaqouri@uhp.ac.ma*

Abstract

While numerous techniques have been proposed to improve the mechanical contact performance of disc brakes during single-stop braking. The aim of this numerical study is to investigate the effect of disc material on the mechanical performance of brake pads. Therefore, a mechanical analysis with COMSOL Multiphysics 6.1 software is performed on two types of solid disc materials: Inconel 718 and grey cast iron using the same model of calculation. The calculation was examined using the FE method. This analysis was carried out to determine wear depth, wear rate, Von Mises stress on the disc and contact pressures during single-stop braking. The results indicate significant differences in mechanical performance as a function of disc material properties. INCONEL 718 showed the lowest wear rate, while grey cast iron showed the lowest Von Mises stress due to their mechanical properties. These results confirm the importance of disc material in optimising brake pad performance.

***Keywords*:** wear depth, von Mises stress, disc, pad, single-stop braking.
PACS numbers: 46.55.+d, 81.40.Pq, 81.40.Np

Received:	*Revised:*	*Accepted:*	*Published:*
9 September 2025	*15 November 2025*	*18 February 2026*	*31 May 2026*

1. Introduction

With Optimal design requires the use of efficient and cost-effective technologies available to solve engineering problems, as well as experimental studies. In the automotive and aerospace sectors, many parts have to cope with concurrent thermal and mechanical loads, which may be fluctuating or constant. The thermomechanical stresses cause deformations that can even deteriorate the system. Friction braking systems, in particular, generate heat in the brake disc and pads, leading to high stresses, deformation and vibration [1-6].

In the literature, Johansson [7] is among the first authors to evaluate wear in a numerical simulation; employing the finite element method (FEM), he investigated the contact pressure between two bodies when the material is subjected to frictional wear, proposing the fundamental equations in a discrete way to calculate local wear on the basis of Archard's law. Molinari and al [8] generalised Archard's law to some extent to introduce features such as the temperature dependence of hardness, thus capturing transitions in the wear regime. McColl and al [9] used 2D finite element modelling in ABAQUS to determine the frictional contact of a cylinder on a flat fretting test, using a modified version of Archard's equation for sliding wear. Soderberg and Andersson [10] examined the contact between the pad and rotor of car disc brakes as a compliant dry sliding contact to determine pressure and wear, using ANSYS

and Archard's macro-scale phenomenological wear law. Shinde and Borkar [11] carried out an analysis of the brake disc system using ANSYS software to investigate the performance of two different pad materials: ceramic and fiber composite. This study has made it possible to develop design tools to improve the braking system performance according to stiffness and strength criteria. Dhiyaneswaran [12] conducted a comparative study of the disc brake using two different materials. The brake disc system was analysed under dynamic loading conditions. The displacements and elastic stresses of existing and alternative disc brake materials were also compared. Abdullah and al [13] employed the finite element method to examine the contact pressure and stresses during the period of full clutch engagement using different contact algorithms. This study revealed the sensitivity of the contact pressure results by showing the importance of the contact stiffness between the contact surfaces. Belhocine and al [14] studied the stress concentrations, structural deformations and contact pressure of the brake disc and pads during single-stop braking using ANSYS 11.0. The main objective of this paper was to study the contact mechanics and dry sliding behaviour between the brake disc and pads during the Single-Stop Braking using two different materials of disc. The calculation was carried out on the basis of a static analysis of the structure Comsol Multiphysics 6.1 software.

2. Materials and methods

2.1 Geometry

This study analyses a full disk of a light vehicle, and was created using the Comsol Multyphisics. Figure 1 and table 2 show the geometry and dimensions of this discs respectively, while table 1 details the material properties.

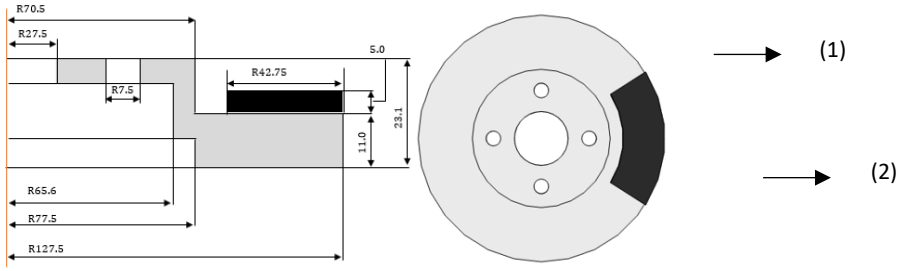

Figure 1. Section of the disc brake model and dimensions. (1) the rotor, (2) the pad

Material Properties	Grey Cast Iron[15]	Inconel 718 AISI [16]	Pad Material
Density (kg.m^{-3})	7850	8220	1400
Young's modulus (GPa)	98	200	1
Poisson's ratio	0.27	0.29	0.42

Table 1. Values of the material properties

Parameters	**Value**
Friction coefficient	0.35
Arc angle pad	65^0
Disc contact surface, Sd (m^2)	0.032079
Pad contact surface, Sp (m^2)	0.005148
Initial angular velocity(rad.s^{-1})	155.54
Pressure p (MPa)	1.4
Time braking	4

Table 2. Values of the numerical parameters

3. Modelling mechanical problems

3.1 Wear calculation procedure

The modelling used mainly treats the wear phenomenon locally by situating particular points on the friction surfaces in order to determine a correlation between the wear depth *W* at a specific point and the sliding distance *s* of this point with respect to the interacting surface. Wear is analysed as a dynamic process. In this case, the wear model is of the form [10]:

$$\frac{\partial W}{\partial t} = f(load, Velocity, Temp, Material) \tag{1}$$

The interface between the rotor and the insert can be considered as a dry sliding contact. The most commonly applied model for predicting sliding contact wear is Archard's linear wear law [17]. This law can be generalised by the fact that the rate of wear at each point on the friction surface depends on the relative sliding speed V_{slip} and the local contact pressure p_n, by applying the following formula:

$$\frac{\partial W}{\partial t} = k_{wear}\left(\frac{p_n}{p_{ref}}\right)|\omega_0.r| \tag{2}$$

P_{ref} designates the reference contact pressure and is used to obtain coherent units. K_{wear} designates a wear constant and the exponent n regulates the dependency of the wear rate on the contact pressure. With $n = 1$ and $p_{ref} = 1Pa$, the relative slip velocity, V_{slip}, is calculated as follows: $V_{slip}=|\omega_0.r|$.

In this study the contact pressure is triggered by adding a boundary load to the upper surface of the brake pad, while friction forces are used to determine the relative sliding speed between rotor and pad. The brake disc is assumed to have an angular velocity $\omega = \omega(t)$. At each point on the working surface, during braking, the depth of wear of the friction material is calculated continuously according to Archard's law [17].

3.2 Procedure for calculating contact pressure

Using the augmented Lagrangian formulation for normal contact, the pressure distribution pn is obtained. This formulation, in a weak sense, applies the non-penetration condition precisely beyond the limits of the contact surface. It is calculated as follows increase in:

$$0 = \cdots + \int_{T_{pad}} \rho_{np}\delta g_n dS_c - \frac{1}{\varepsilon_n}\int_{T_{pad}}(p_{np} - p_n)\,\delta p_n dS_c \tag{3}$$

Where p_{np} denotes the penalised (or increased) contact pressure and p_n a Lagrange multiplier or the contact pressure, g_n represents the geometric distance. It is important to note that g_n is not always the nearest distance separating both limits' boundaries.

The Lagrange multiplier representing the dependent variable of the contact problem and is usually discretised by Lagrangian shape functions.

The segregate method, which corresponds to what is known as the Uzawa algorithm, is used to solve the system of coupled equations mentioned above. the resolution of the Lagrange multiplier and the displacement field is carried out separately of each other. Consequently, the solver has two iteration levels, where p_n is maintained constant when u is solved, and inversely when p_n is updated. p_{np} for the outer iteration $j+1$ is calculate by:

$$\begin{cases} p_{np,j+1} = p_{n,j} - \varepsilon_n g_n \quad if \;\; g_n \le 0 \\ p_{np,j+1} = p_{n,j} - e^{\varepsilon_n g_n / p_n} \quad else \end{cases} \tag{4}$$

3.3 Meshing

The quadratic serendipity mode was chosen for the construction of the model presented. The selection of this mode reduced the computation time. In total, the braking system mesh comprised 3759 tetrahedral elements, 2492 triangular elements and 590 edge elements (figure 2).

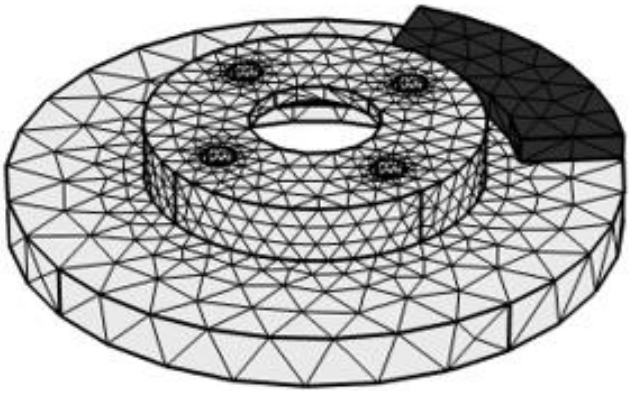

Figure 2. Mesh elements of the model

4. Results and discussion

4.1 Influence of material on brake pad wear depth

These results analyse the mechanical behaviour of two cases, each one from a different material: Inconel 718 and grey cast iron. A transient mechanical model, Archard, was used to calculate the maximum wear depth over time and to define the contours of the wear distribution.

Figure 3 shows the evolution of the wear depth during the braking phase and for two calculation cases. This curve illustrates that the wear depth rises gradually until its maximum value $W_{1max} = 133\ \mu m$ *and* $W_{2max} = 91\ \mu m$ respectively. The result shows the importance of disc material in optimising brake pad performance.

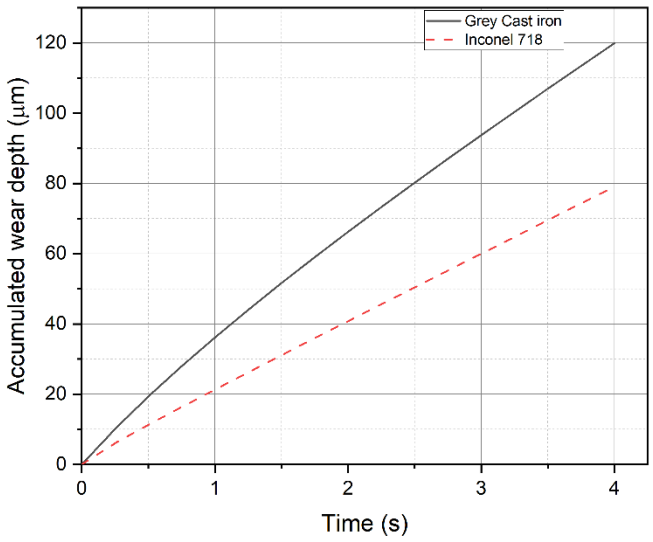

Figure 3. The wear depth evolution at two distinct discs material

Figure 4 a,b shows the spatial variations in wear depth for the two cases at end time of simulation . The maximum value of wear depth is located in the contact region, specifically in the pad attack region of system and at the maximum radius.

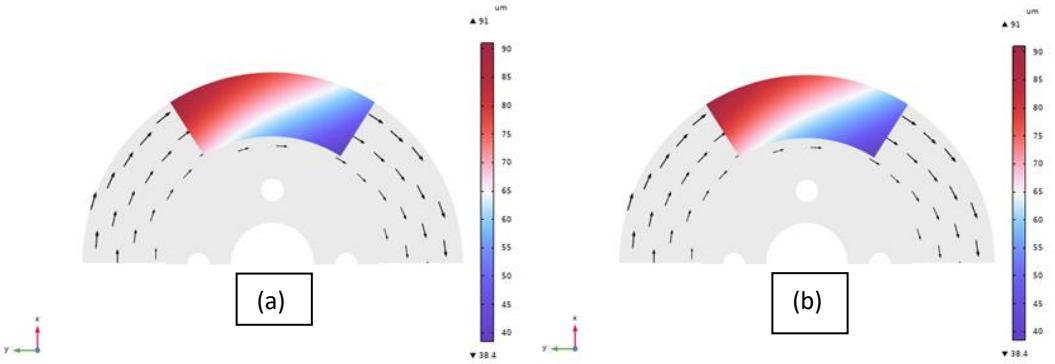

Figure 4. Wear depth distribution on pad for two distinct disc's materials. a) cast iron, b) inconel780

4.2 Influence of material on pad's von mises stress profiles

Figure 5 illustrates the von mises spatial stress distribution for pad. It can be observed very clearly that the maximum stress at the contact surface of the pad can reach a value of 2.63 MPa and 3.58 MPa for the two cases respectively. In addition, figure 6 shows the variation in stress along the thickness of the rotor disc. The result shows that the maximum stress value is located in the zone where the tracks connect to the bowl and at the mounting holes, with a maximum value of 25 MPa in both cases.

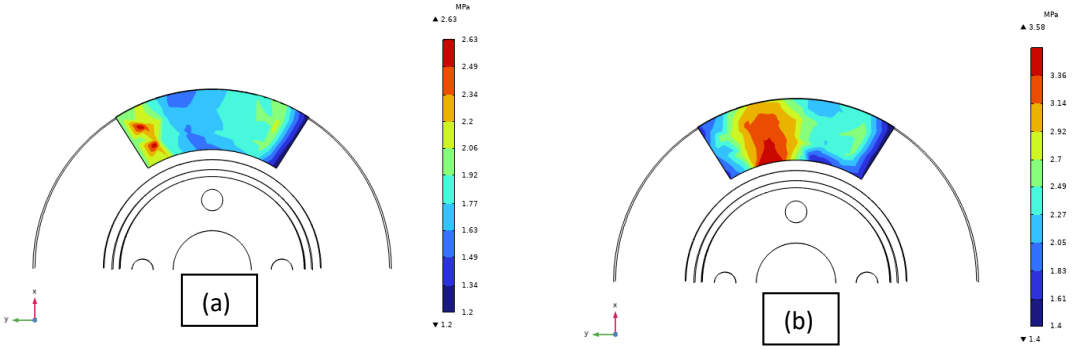

Figure 5. Stress pad distributions taken at two distinct disc's materials. a) cast iron, b) inconel780

Figure 6. The stress distributions taken at two distinct disc's materials. a) cast iron, b) inconel780

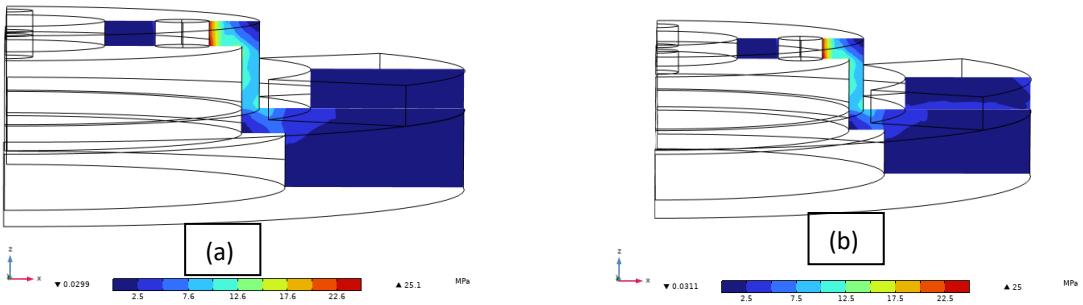

4.3 Influence of material on pad's contact pressure profiles

If frictional forces are taken into account, the contact pressure is more important at the leading-edge zone of the pad (figure 7). Nevertheless, in the case where no friction is involved in the contact between the pad and the disc, there would be a symmetrical distribution of the value of the contact pressure. It can be observed very clearly in figure 8 that the maximum contact pressure at the start of braking at $P_{1max} = 3.5\ MPa$ and $P_{2max} = 3.65\ MPa$ for the two

cases respectively, then its gradual full to a minimum value P_{1min}= *2.23MPa* and P_{2min}= *1.73MPa.*

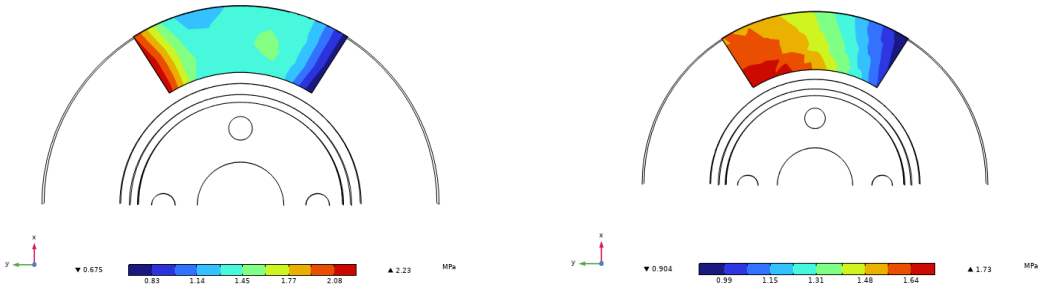

Figure 7. Contact pressure distributions at two disc's materials. a) cast iron, b) Inconel780

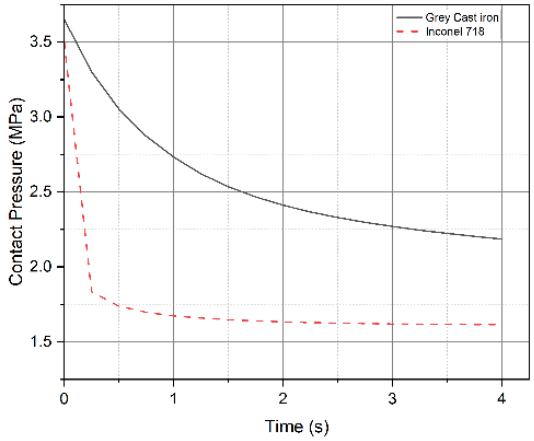

Figure 8. The contact pressure evolution at two disc's materials

4.4 Influence of disc rotation speed on pad brake wear depth

The increase in disc rotation speed raises the contact pressures and stresses as well as the wear depth of the pads. The evolution of the wear depth for different speeds of rotation is shown in figure 9. It can be seen that the wear depth remains proportional to the speed of rotation and when the speed is increased from 80 to 140 km/h, the wear depth increases 4 times the initial value.

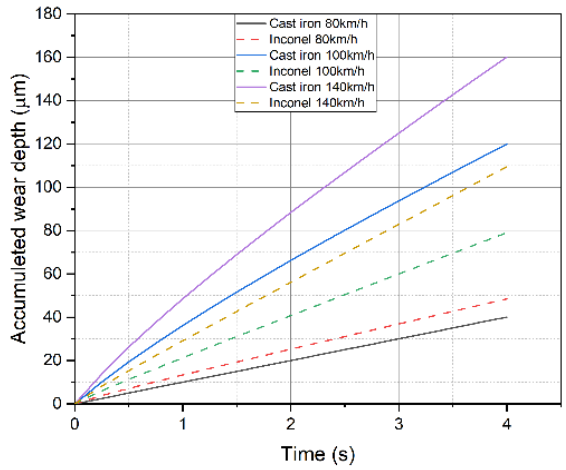

Figure 9. The evolution of the wear depth of pad at two distinct disc's speed disc rotation.

5. Conclusion

The present work presents an analysis of the purely mechanical dry contact between two different bodies (disc/pad). Using the same model developed and modifying only the rotor material, the FE method was used to examine the calculation and the results are summarised as follows: The use of grey cast iron material has a positive effect on pad surface stress; stress concentration is generally high in the disc bowl and friction grid, which can lead to mechanical faults such as wear, radial cracking and rupture; the disc material selection is based on its Young's modulus. Inconel 718, which has the highest Young's modulus, reduces contact pressure and therefore wear depth, resulting in a reduction in the wear rate of the insert. The increase in disc rotation speed raises the contact pressures and stresses as well as the wear depth of the pads.

Acknowledgment

Thanks to Maniana M and Tajmouati A for their writing guidance and for his theoretical guidance.

References

1. G. Cueva, A. Sinatora, W.L. Guesser, and A.P. Tschiptschin, Wear **255**(7–12) (2003) 1256.
2. S. Zhao, G.E. Hilmas, and L.R. Dharani, Carbon **47**(9) (2009) 2219.
3. S. Zhao, G.E. Hilmas, and L.R. Dharani, Wear **264**(11–12) (2008) 1059.
4. M. Chaqouri, M. Maniana, and A. Tajmouati, International Journal of Information Science and Technology **8**(3) (2024) 21.
5. M. Chaqouri, M. Maniana, and A. Tajmouati, Influence of Pad Geometry on the Mechanical Study of a Disc Brake, in Proc. 2024 4th International Conference on Innovative Research in Applied Science, Engineering and Technology (IRASET), IEEE (2024) 01.
6. M. Maniana, M. Chaqouri, S. Benkachcha, and A. Tajamouati, Thermomechanical Study of a Disc Brake, in Proc. 2023 3rd International Conference on Innovative Research in Applied Science, Engineering and Technology (IRASET), IEEE (2023) 1.
7. L. Johansson, Numerical Simulation of Contact Pressure Evolution in Fretting, ASME J. Tribol. **116**(2) (1994) 247.
8. J.F. Molinari, M. Ortiz, R. Radovitzky, and E.A. Repetto, Engineering Computations **18**(3/4) (2001) 592.
9. I.R. McColl, J. Ding, and S.B. Leen, Wear **256**(11–12) (2004) 1114.
10. Söderberg and S. Andersson, Wear **267**(12) (2009) 2243.
11. N.B. Shinde and B.R. Borkar, J. Eng. Comput. Sci. **4**(3) (2015) 10697.
12. S. Dhiyaneswaran and K.S. Amirthagadeswaran, Int. J. Mod. Eng. Res. (2014) 173.
13. O.I. Abdullah, J. Schlattmann, and A.M. Al-Shabibi, Tribology in Industry **35**(2) (2013) 155.
14. A. Belhocine, A.R. Abu Bakar, and O.I. Abdullah, Trans. Indian Inst. Metals **68** (2015) 403.
15. J. Wahlström, A comparison of measured and simulated friction, wear, and particle emission of disc brakes, Tribology International **92** (2015) 503.
16. B. Onuike and A. Bandyopadhyay, Additive manufacturing of Inconel 718–Ti6Al4V bimetallic structures, Additive Manufacturing **22** (2018) 844.
17. A. Rudnytskyj, Diss: Simulations of contact mechanics and wear of linearly reciprocating block-on-flat sliding test (2018).